arXiv:cond-mat/0510301v2 [cond-mat.mes-hall] 28 May 2006

Phase Separation of a Fast Rotating Boson-Fermion Mixture in the Lowest-Landau-Level Regime

Rina Kanamoto * and Makoto Tsubota
Department of Physics, Osaka City University, Osaka 558-8585, Japan
(Dated: February 2, 2008)

By minimizing the coupled mean-field energy functionals, we investigate the ground-state properties of a rotating atomic boson-fermion mixture in a two-dimensional parabolic trap. At high angular frequencies in the mean-field-lowest-Landau-level regime, quantized vortices enter the bosonic condensate, and a finite number of degenerate fermions form the maximum-density-droplet state. As the boson-fermion coupling constant increases, the maximum density droplet develops into a lower-density state associated with the phase separation, revealing characteristics of a Landau-level structure.

PACS numbers: 03.75.Hh, 03.75.Lm, 03.75.Ss

Experimental developments in the cooling techniques of atomic gases have provided new opportunities to investigate the quantum-degenerate regime where Bose-Einstein condensations (BECs), Fermi-Dirac (FD) degeneracies [1, 2], and BECs of paired states emerge [3, 4]. The heteronuclear Feshbach resonance, which was recently found in a boson-fermion mixture [5], also enables us to investigate the quantum-statistical origin of novel phenomena. This system sheds light not only on our understanding of boson-mediated pairing of fermions [6], but also on the relationship to condensed matter physics [7], multicomponent systems [8], and the study of the normal and superfluid states of fermions [9].

When a superfluid system is subjected to an external rotating drive above a critical angular frequency, the system forms quantized vortices, which are experimentally observed both in bosonic [10] and paired fermionic [11] systems. On the other hand, a number of analogies have been pointed out between neutral atoms subjected to an external rotation and charged particles in a magnetic field [12, 13, 14] regardless of quantum statistics of atoms. As an example, a finite number of electrons in a quantum dot (QD) (e.g., realized in a semiconductor heterostructure) form the maximum density droplet (MDD) state [15], reflecting the lowest-Landau-level (LLL) structure of electrons under a strong magnetic field. In the MDD, the total angular momentum of electrons takes the lowest possible value due to the FD degeneracy and the Pauli exclusion principle. However, the interplay between the Pauli pressure plus potential term and the electron-electron interaction causes an instability against density modulation or edge reconstruction [16, 17]. Such reconstructions are expected to emerge in the spin-polarized fermions under fast rotation.

In this Letter, we address the boson-fermion mixture, and show that reconstruction process is associated with a phase separation between components due to the significance of repulsive boson-fermion interaction in the fast-rotating regime. For larger external angular frequency the components separate at smaller interaction, and the increase in the angular momentum of fermions from one of the MDD state is quantized at the integral multiple of the total number of fermions after phase separation. However, this quantization can be violated at the phase-coexistent regime as a consequence of the rotational symmetry breaking of the BEC with a vortex lattice.

We consider the gaseous atomic mixture of $N_{\rm B}$ bosons and spin-polarized $N_{\rm F}$ fermions in a parabolic trap which rotates around the z axis. When the angular frequencies of the trap are highly anisotropic as $\omega_z \gg \omega_{x,y} \equiv \omega$, the atomic motion virtually reduces to two-dimensional (2D). The trapping frequencies and atomic masses for the two components are assumed to be identical, being denoted as ω and M. Henceforth, the angular momenta, energies, and lengths are measured in units of $\hbar$, $\hbar\omega$, $l = \sqrt{\hbar/(M\omega)}$, respectively.

The low-energy scatterings are characterized by s-wave scatterings which are modeled by contact interactions. The interaction and correlation between fermions are thus absent because of the Pauli principle. The dimensionless 2D boson-boson and boson-fermion couplings g, h are related to the 3D ones $g_{\rm BB}^{\rm (3D)} = 4\pi\hbar^2 a_{\rm BB}/M$ and $h_{\rm BF}^{\rm (3D)} = 4\pi\hbar^2 a_{\rm BF}/M$, as $g = g_{\rm BB}^{\rm (3D)}/(\sqrt{2\pi}l_z)$ and $h = h_{\rm BF}^{\rm (3D)}/(\sqrt{2\pi}l_z)$ with $l_z = \sqrt{\hbar/(M\omega_z)}$, respectively. We treat the boson-boson interaction and boson-fermion interaction within the mean-field approximation, which is valid for a weakly-interacting system under moderate rotating drive. As the rotating drive increases, both components will enter the *mean-field-lowest-Landau-level* (MF-LLL) regime [18], where the single-particle states are described within the LLL, but the mean-field approximation is still valid [19]. Throughout this paper, we address the regime where the mean-field approximation is expected to be valid.

Let us suppose that the bosons are BE-condensed oc-

*Present address: Department of Physics, The University of Arizona, Tucson, AZ, USA.

cupying a single-particle state $\psi_{\rm B}$, while the fermions are FD-degenerate occupying single-particle orbitals $\psi_{\rm F}^{(j=1,...,N_{\rm F})}$. The mean-field energy functional in the rotating frame is given by

$$E_{\rm B} = N_{\rm B}\int d^2r\psi_{\rm B}^*(\boldsymbol{r})\left[\hat{H}+\frac{g}{2}n_{\rm B}(\boldsymbol{r})\right]\psi_{\rm B}(\boldsymbol{r}), \quad (1)$$

$$E_{\rm F} = \sum_{j=1}^{N_{\rm F}}\varepsilon_{\rm F}^{(j)}; \quad \varepsilon_{\rm F}^{(j)} = \int d^2r\psi_{\rm F}^{(j)*}(\boldsymbol{r})\hat{H}\psi_{\rm F}^{(j)}(\boldsymbol{r}), \quad (2)$$

$$E_{\rm BF} = h\int d^2r n_{\rm F}(\boldsymbol{r})n_{\rm B}(\boldsymbol{r}), \quad (3)$$

where $\hat{H}=(-\nabla^2+r^2)/2-\Omega\hat{L}_z$ is the Hamiltonian for a free atom with $\hat{L}_z=-i(x\partial_y-y\partial_x)$, and Ω is the angular frequency of the external rotating drive in unit of ω. The densities are given by $n_{\rm B}(\boldsymbol{r})=N_{\rm B}|\psi_{\rm B}(\boldsymbol{r})|^2$, and $n_{\rm F}(\boldsymbol{r})=\sum_{j=1}^{N_{\rm F}}|\psi_{\rm F}^{(j)}(\boldsymbol{r})|^2$, where the summation over j is taken over all occupied states of fermions. The eigensolutions of $\hat{H}$

$$\varepsilon_{nm}^{(0)} = n+m+1-\Omega(m-n), \quad n,m=0,1,..., \quad (4)$$

$$u_{nm}(\boldsymbol{r}) = \frac{1}{\sqrt{\pi n!m!}}e^{\frac{r^2}{2}}\left(\partial_x+i\partial_y\right)^m\left(\partial_x-i\partial_y\right)^n e^{-r^2}, \quad (5)$$

are well-defined angular-momentum states, i.e., $\hat{L}_z u_{nm}(\boldsymbol{r})=(m-n)u_{nm}(\boldsymbol{r})$.

We expand the single-particle orbitals as $\psi_{\rm B}(\boldsymbol{r})=\sum_{n,m}b_{nm}u_{nm}(\boldsymbol{r})$, and $\psi_{\rm F}^{(j)}(\boldsymbol{r})=\sum_{n,m}f_{nm}^{(j)}u_{nm}(\boldsymbol{r})$, and minimize the total energy with the normalization conditions $\sum_{n,m}b_{nm}^2=\sum_{n,m}f_{nm}^{(j)2}=1$, where b_{nm} and f_{nm} are taken to be real without loss of generality. We then numerically iterate minimization of $\tilde{\varepsilon}_{\rm B}=(E_{\rm B}+E_{\rm BF})/N_{\rm B}$ and diagonalization of $\tilde{\varepsilon}_{\rm F}=\varepsilon_{\rm F}+h\int d^2r\psi_{\rm F}^*n_{\rm B}\psi_{\rm F}$ until they self-consistently converges [20, 21]. Since we use the mean-field approximation, we find a relevant breaking of rotational symmetry in the density distributions without investigating higher-order correlation functions.

The ground-state angular momentum of each component is shown in Fig. 1 as a function of Ω. The total angular momentum of the BEC, $L_{\rm B}=N_{\rm B}\sum_{n,m}b_{nm}^2(m-n)$, remains zero associated with the superfluidity. For fermions, in contrast, $L_{\rm F}=\sum_{j=1}^{N_{\rm F}}\sum_{n,m}f_{nm}^{(j)2}(m-n)$ increases as Ω exceeds zero. Within the semiclassical description with the rigid-body rotation, the total angular momentum of free fermions is given by $L_{\rm F}^{\rm (RB)}=\Omega\int r^2n_{\rm F}(\boldsymbol{r})d^2r=(8N_{\rm F})^{3/2}\Omega/(24\sqrt{1-\Omega^2})$. This function is plotted with the dashed curve in Fig. 1, and is found to agree well with $L_{\rm F}$ for slow rotating regime. The semiclassical theory of a free fermi gas is therefore good [22] even when fermions weakly interact with bosons.

As the angular frequency of the external rotating drive increases, $L_{\rm B}$ jumps from zero to $N_{\rm B}$ at

$$\Omega_{\rm cr}^{\rm (B)} = 1-G-2b_{11}^2-2Gb_{11}[b_{11}-(1+b_{00}^2)b_{00}] \quad (6)$$

where $G\equiv gN_{\rm B}/(8\pi)$, and $b_{11}^2=G^2/(8G^2+2G+1)$, $b_{00}^2=1-b_{11}^2$ [23]. This jump corresponds to the onset of vortex formation in the BEC. The dominant contributions to $\Omega_{\rm cr}^{\rm (B)}$ are the first two terms which coincide with the result within the LLL approximation. The remaining terms arise from the higher Landau levels which are almost negligible as compared with the first two terms, but modify $\Omega_{\rm cr}^{\rm (B)}$ as g increases. We find from the numerical and variational calculations that the BEC with $gN_{\rm B}\lesssim O(1)$ enters the MF-LLL regime in $\Omega\gtrsim\Omega_{\rm cr}^{\rm (B)}$ where the quantized vortices successively form in the BEC.

For fermions the semiclassical description fails in a fast-rotating regime because the energy-level discreteness becomes crucial. This is shown in Fig. 1 (b), where the emergence of the plateau at $L_{\rm F}^{\rm (MDD)}$ and the significant deviation from $L_{\rm F}^{\rm (RB)}$ are the manifestations of the fact that fermions enter the LLL regime. The degenerate fermions occupy from the lowest level $m=0$ up to the highest level $m=N_{\rm F}-1$ in the LLL according to the Pauli principle, and hence $L_{\rm F}$ is frozen at the value $L_{\rm F}^{\rm (MDD)}=N_{\rm F}(N_{\rm F}-1)/2$ whereas $L_{\rm F}^{\rm (RB)}$ diverges. The order of Ω at which the fermions cross over from the semiclassical to a quantum regime is estimated by the condition $L_{\rm F}^{\rm (RB)}=L_{\rm F}^{\rm (MDD)}$, as

$$\Omega_{\rm cr}^{\rm (F)} = \frac{3(N_{\rm F}-1)}{\sqrt{9N_{\rm F}^2+14N_{\rm F}-9}}, \quad (7)$$

which approaches unity in the limit $N_{\rm F}\to\infty$.

On the $L_{\rm F}^{\rm (MDD)}$-plateau the fermionic density becomes maximum, which is thus called a MDD in QDs with a finite number of electrons [15]. The area occupied by fermions becomes minimum since the mean-radius of the LLL orbital is given by $\langle r^2\rangle_m=m+1$. The MDD state is the trivial ground state of free fermions in the MF-LLL regime, and is regarded as the fermionic counterpart of

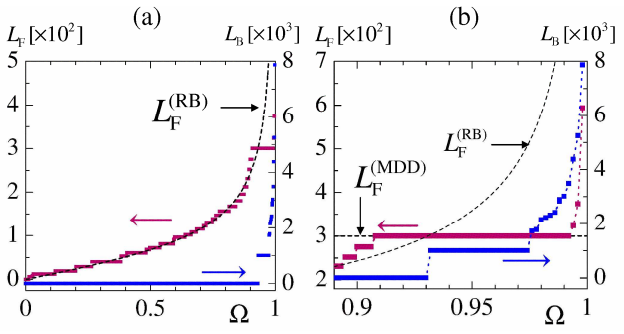

FIG. 1: (color online) Total angular momentum of each component with $N_{\rm B}=1000, N_{\rm F}=25$, and $g=0.5h=2\times10^{-3}$. (a) Plateau at zero in $L_{\rm B}$ arises from the irrotationality. Small steps in $L_{\rm F}$ arise from the size effect. These steps become invisible for larger $N_{\rm F}(\gtrsim 500)$. (b) Enlargement of (a) for the fast-rotating regime.

a BEC without a quantized vortex in terms of the angular momentum [13]. The corresponding many-body wave function of fermions is given by the Slater determinant constructed by the LLL orbitals $\psi_{\rm F}^{(j)}(\boldsymbol{r}) = u_{0m}(\boldsymbol{r})$ for $m = 0, 1, \ldots N_{\rm F} - 1$, which is shown to be reduced to the Laughlin wave function of the integer quantum Hall state with $\nu = 1$,

$$\Psi_{\rm F}^{(0)}(\mathcal{Z}_1, \mathcal{Z}_2, \ldots, \mathcal{Z}_{N_{\rm F}}) = \prod_{i<j}(\mathcal{Z}_i - \mathcal{Z}_j) \exp\left(-\sum_k \frac{|\mathcal{Z}_k|^2}{2}\right), \tag{8}$$

where $\mathcal{Z} \equiv x + iy$. In the absence of the boson-fermion interaction, $L_{\rm F}$ remains $L_{\rm F}^{\rm (MDD)}$ for $\Omega \geq \Omega_{\rm cr}^{\rm (F)}$. In the presence of the boson-fermion interaction, however, $L_{\rm F}$ begins to increase in the limit $\Omega \to 1$ as shown in Fig. 1 (b). This behavior features a phase separation caused by the boson-fermion interaction, and is *not* the reminiscent of the divergence in $L_{\rm F}^{\rm (RB)}$ of free fermions. In the same manner as the nonlinear interaction of the BEC leads to the successive formation of quantized vortices, the boson-fermion interaction also induces the successive penetration of fluxes of angular momenta in the fermionic cloud.

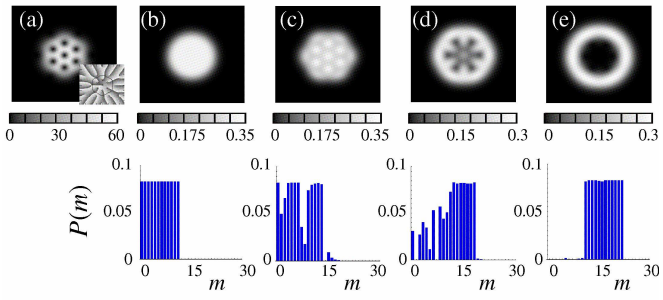

FIG. 2: (color online) (a) Density, and phase (inset) profiles of the bosonic condensate wave function. (b)-(e) Density profiles (upper panels) and mean angular-momentum distributions (lower panels) of the fermionic cloud for $h/g = 0, 1, 1.5$, and 2.5, respectively.

In order to examine how the boson-fermion coupling modulates the ground state in the MF-LLL regime, we henceforth restrict the bases u_{nm} within the LLL, omitting the index n. Typical density profiles for several values of h are shown in Fig. 2 where other parameters are fixed to be $\Omega = 0.995, N_{\rm B} = 1000, N_{\rm F} = 12$, and $g = 2 \times 10^{-3}$. The number of quantized vortices remains unchanged, and hence the condensate wave function looks like ones shown in Fig. 2 (a) throughout the increase in h. In contrast, the fermionic density $n_{\rm F}$ changes drastically as h increases. The histograms show the mean angular-momentum distribution of fermions defined by $P(m) \equiv \sum_{j=\rm occ} |f_m^{(j)}|^2/N_{\rm F}$, which is equal to $1/N_{\rm F}$ for $0 \leq m \leq N_{\rm F} - 1$ in the MDD state [(b)]. When the weak interaction is introduced [(c)], the occupations of some low-angular-momentum states begin to be partially shifted to higher-angular-momentum states which are not occupied in the MDD state. The fermionic density increases in the vortex cores of the condensate, breaking the rotational symmetry in order to reduce the repulsive interaction energy. The derivation from the homogeneous distribution $1/N_{\rm F}$ in $P(m)$ is a signal of the rotational symmetry breaking. As h increases further [(d)], more angular-momentum states are shifted, and the region where components overlap gradually decreases. The bosonic and fermionic densities eventually separate for larger values of h, where a large central hole emerges in the fermionic cloud [(e)]. The mean angular-momentum distribution again becomes uniform with the value $1/N_{\rm F}$ for $M \leq m \leq M + N_{\rm F} - 1$, and the rotational symmetry in $n_{\rm F}$ is recovered independent of the configuration of the vortex lattice in the BEC. This state is regarded as the penetration of M fluxes of angular momenta in the MDD state. Such a quasi-1D-like density and corresponding angular-momentum distribution also occur in the case of free fermions in $\Omega \gtrsim 1$ with an elimination of the centrifugal singularity [12, 24].

We next study the changes in the total angular momentum of each component and the boson-fermion interaction energy associated with the phase separation in the MF-LLL regime. In Fig. 3 we show $\tilde{L}_{\rm B} \equiv L_{\rm B}/N_{\rm B}$, $\tilde{L}_{\rm F} \equiv (L_{\rm F} - L_{\rm F}^{\rm (MDD)})/N_{\rm F}$, and $E_{\rm BF}$ for several values of Ω and $N_{\rm F}$, with $g = 2 \times 10^{-3}$ and $N_{\rm B} = 10^3$

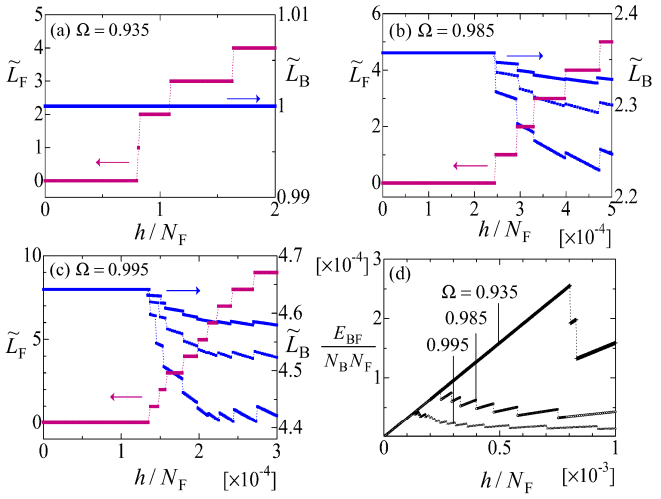

FIG. 3: (color online) (a)-(c) Total angular momentum of each component for three values of Ω. Three plots of $\tilde{L}_{\rm B}$ in each panel denote the results with $N_{\rm F} = 32, 64, 128$ from top down. The plateaus in $\tilde{L}_{\rm F}$ are located at zero or positive integers. (d) Boson-Fermion interaction energy $E_{\rm BF}$. Jumps in $\tilde{L}_{\rm B}$, $\tilde{L}_{\rm F}$, and $E_{\rm BF}$ occur at the same values of $h/N_{\rm F}$ for a fixed Ω.

$h/N_{\rm F}$. Before the phase separation, $\tilde{L}_{\rm B}$ and $\tilde{L}_{\rm F}$ are nearly constant and $E_{\rm BF}$ linearly increases with $h/N_{\rm F}$. At a critical value $h/N_{\rm F}$ where $E_{\rm BF}$ becomes maximum, the phase separation occurs and fermions begin to rotate around the BEC. Since the boson-fermion interaction becomes significant for larger Ω, the critical value of interaction h becomes smaller for a faster rotating drive. After the phase separation, the system is well described in terms of *noninteracting* fermion model, because the fermions recover the rotational symmetry after phase separation and the value $P(m)$ cannot deviate from $1/N_{\rm F}$. The angular-momentum states of fermions in the phase-separating regime are therefore regarded as states where some angular-momentum fluxes penetrate the MDD. Let us define M as the number of fluxes of angular momentum where the fermions homogeneously occupy the single-particle states ranging from $m = M$ to $m = M + N_{\rm F} - 1$. The difference between the total angular momentum of fermions $L_{\rm F}^{(M)}$ with M fluxes and one of the MDD state is given by

$$L_{\rm F}^{(M)} - L_{\rm F}^{(\rm MDD)} = \sum_{m=M}^{M+N_{\rm F}-1} m - \sum_{m=0}^{N_{\rm F}-1} m = MN_{\rm F}. \quad (9)$$

The corresponding many-body wave function of fermions with the angular momentum $L_{\rm F}^{(M)}$ is constructed by successive multiplications of the symmetric polynomial

$$\mathcal{S}(\mathcal{Z}_1, \mathcal{Z}_2, \ldots, \mathcal{Z}_{N_{\rm F}}) = \prod_j \mathcal{Z}_j \quad (10)$$

to the MDD state $\Psi_{\rm F}^{(0)}$ given by Eq. (8), where the antisymmetry of the fermionic wave function is ensured by $\Psi_{\rm F}^{(0)}$ [25]. The polynomial $\mathcal{S}$ increases the angular momentum of each fermion by one, and the change in the total angular momentum $L_{\rm F}$ is thus given by $N_{\rm F}$. Upon the increase in M, the boson-fermion interaction energy $E_{\rm BF}$ decreases discontinuously as shown in Fig. 3 (d). The total angular momentum of bosons is partially transferred to fermions only when the number of quantized vortices in the BEC is larger than unity, and the number of vortices remains unchanged. On the other hand, the radius of fermionic cloud increases with M, while the rotational symmetry of the annular density profile is kept as shown in Fig. 2(e).

In conclusion, we have studied the phase separation between spin-polarized fermions and the BEC at high angular frequency in the MF-LLL regime. The ground-state reconstruction has been found in the density profiles, angular momenta, and boson-fermion interaction energy. We have shown that this reconstruction associated with the phase separation can be understood in terms of successive penetration of the angular-momentum fluxes to the fermionic cloud. We acknowledge Akira Oguri for fruitful discussion and comments.

[1] A.G. Truscott *et al.*, Science **291**, 2570 (2001); F. Schreck *et al.*, Phys. Rev. Lett. **87**, 080403 (2001).
[2] B. DeMarco and D.S. Jin, Science **285**, 1703 (1999).
[3] E.A. Donley *et al.*, Nature (London) **417**, 529 (2002).
[4] K.M. O'Hara *et al.*, Science **298**, 2179 (2002); C.A. Regal *et al*, Nature (London) **424**, 47 (2003).
[5] S. Inouye *et al.*, Phys. Rev. Lett. **93**, 183201 (2004).
[6] M.J. Bijlsma, B.A. Heringa, and H.T.C. Stoof, Phys. Rev. A **61**, 053601 (2000); J. Tempere *et al.*, Phys. Rev. B **72**, 094506 (2005).
[7] L. Mathey *et al.*, Phys. Rev. Lett. **93**, 120404 (2004); M. Cramer, J. Eisert, and F. Illuminati, Phys. Rev. Lett. **93**, 190405 (2004); T. Miyakawa, H. Yabu, and T. Suzuki, Phys. Rev. A **70**, 013612 (2004); M. Salerno, Phys. Rev. A **72**, 063602 (2005).
[8] C. Ospelkaus, et el., Phys. Rev. Lett. **96**, 020401 (2006); T. Karpiuk *et al.*, Phys. Rev. Lett. **93**, 100401 (2004).
[9] A. Minguzzi and M.P. Tosi, Phys. Rev. A **63**, 023609 (2001); C.P. Search *et al.*, Phys. Rev. A **65**, 063615 (2002); M. Cozzini and S. Stringari, Phys. Rev. Lett. **91**, 070401 (2003); G. Tonini and Y. Castin, e-print cond-mat/0504612.
[10] K.W. Madison *et al.*, Phys. Rev. Lett. **84**, 806 (2000); J.R. Abo-Shaeer *et al.*, Science **292**, 476 (2001).
[11] M.W. Zwierlein *et al.*, Nature (London) **435**, 1047 (2005).
[12] T.-L. Ho and C.V. Ciobanu, Phys. Rev. Lett. **85**, 4648 (2000).
[13] M. Toreblad *et al.*, Phys. Rev. Lett. **93**, 090407 (2004).
[14] N.K. Wilkin and J.M.F. Gunn, Phys. Rev. Lett. **84**, 6 (2000).
[15] A.H. MacDonald *et al.*, Aust. J. Phys. **46**, 345 (1993).
[16] S.M. Reimann *et al.*, Phys. Rev. Lett. **83**, 3270 (1999).
[17] C. de C. Chamon and X.G. Wen, Phys. Rev. B. **49**, 8227 (1994).
[18] U.R. Fischer and G. Baym, Phys. Rev. Lett. **90**, 140402 (2003); T.-L. Ho, Phys. Rev. Lett. **87**, 060403 (2001); G. Baym and C.J. Pethick, Phys. Rev. A **69**, 043619 (2004).
[19] For free bosons and free fermions of $N_{\rm B} = N_{\rm F} \equiv N$, the angular-momentum states are mapped as $L_{\rm F} = L_{\rm B} + N(N-1)/2$ each other. For weakly-interacting system, the MF-LLL regime for bosons corresponds to $O(N_{\rm B}) \lesssim L_{\rm B} \ll O(N_{\rm B}^2)$. This regime is mapped for fermions as $O(N_{\rm F}^2) \lesssim L_{\rm F} \ll O(N_{\rm F}^3)$, which is roughly expected to be a MF-LLL regime for fermions.
[20] D.A. Butts and D.S. Rokhsar, Nature (London) **397**, 327 (1999); G.M. Kavoulakis, B. Mottelson, and C.J. Pethick, Phys. Rev. A **62**, 063605 (2000).
[21] T. Karpiuk, M. Brewczyk, and K. Rzążewski, Phys. Rev. A **69**, 043603 (2004).
[22] D.A. Butts and D.S. Rokhsar, Phys. Rev. A **55**, 4346 (1997).
[23] This is derived with the assumption $h = 0$. We have confirmed numerically that the boson-fermion interaction hardly affects $\Omega_{\rm cr}^{(\rm B)}$ while the boson-boson interaction is crucial.
[24] A.L. Fetter, Phys. Rev. A **64**, 063608 (2001); E. Lundh, Phys. Rev. A **65**, 043604 (2002); K. Kasamatsu, M. Tsubota, and M. Ueda, Phys. Rev. A **66**, 053606 (2002); V. Bretin *et al.*, Phys. Rev. Lett. **92**, 050403

(2004).
[25] A.H. MacDonald, e-print cond-mat/9410047.